$$\text{Complementarity}: \sum_{j=1}^{N} C_{(i,j),(i,j)}(\tau_1, \tau_2) = 0$$

$$1 \leq i \leq M, \tau_1 \neq 0 \text{ and } \tau_2 \neq 0 \tag{4}$$

$$\text{Orthogonality}: \sum_{j=1}^{N} C_{(i,j),(k,j)}(\tau_1, \tau_2) = 0$$

$$1 \leq i, k \leq M \text{ and } i \neq k, \forall \tau_1, \tau_2 \tag{5}$$

where $C_{(i,j),(k,l)}$ denotes the aperiodic correlation function between array $B_{i,j}$ and $B_{k,l}$.

To obtain the required ZCZ arrays, a recursive formula is needed as shown below:

$$A = \begin{bmatrix} BB & (-B)B \\ (-B)B & BB \end{bmatrix} \tag{6}$$

where $-B$ denotes the matrix whose i,jth entry is the negation of the i,jth of B, BB (or $(-B)B$) denotes the matrix whose i,jth entry is the concatenation of the i,jth entry of B (or $-B$) and the i,jth entry of B.

It is clear that the set A contains $2M$ arrays of order $L_1 \times (2L_2 * 2N)$. Let $A^{(s)}$ and $A^{(t)}$ be two arbitrary arrays, their correlation function satisfying

$$\begin{aligned} R_{s,s}(\tau_1, \tau_2) = 0 \quad & 1 \leq s \leq 2M, |\tau_1| < L_1, |\tau_2| < L_2 + 1 \\ & \text{and } (\tau_1, \tau_2) \neq (0, 0) \\ R_{s,t}(\tau_1, \tau_2) = 0 \quad & 1 \leq s, t \leq 2M, s \neq t, |\tau_1| < L_1 \\ & \text{and } |\tau_2| < L_2 + 1 \end{aligned} \tag{7}$$

That is, the set A is a ZCZ-((L_1, $2L_2 * 2N$), $2M$, (L_1, $L_2 + 1$)) set with $Z_{cz} = (L_1, L_2 + 1)$. Obviously, the set A^T is a ZCZ-(($2L_2 * 2N$, L_1), $2M$, ($L_2 + 1$, L_1)) set with $Z_{cz} = (L_2 + 1, L_1)$, where the superscript T denotes matrix transposition.

Besides, if A is viewed as a set containing $2M$ sets, each set have $2N$ arrays of order $L_1 \times 2L_2$, it would be a mutually orthogonal complementary array set.

We now give the following three constructions:

Construction (i): Based on a two-dimensional mutually orthogonal complementary set B, one can construct a ZCZ-((L_1, $2L_2 * 2N$), $2M$, (L_1, $L_2 + 1$)) set A with $Z_{cz} = (L_1, L_2 + 1)$ by employing eqn. 6 directly.

Construction (ii): Denote the matrix A on the left hand side of eqn. 6 as A_0, which is also a mutually orthogonal complementary array set. Then, by replacing B with A_0 in eqn. 6, we can obtain a new ZCZ array set A_1, i.e. ZCZ-((L_1, $4L_2 * 4N$), $4M$, (L_1, $2L_2 + 1$)) set with $Z_{cz} = (L_1, 2L_2 + 1)$ and size $4M$. Similarly, from a ZCZ array set A_{n-1}, we can construct recursively another new ZCZ array set A_n from A_{n-1}, i.e. ZCZ-((L_1, $2^{n+1}L_2 * 2^{n+1}N$), $2^{n+1}M$, (L_1, $2^nL_2 + 1$)) set with $Z_{cz} = (L_1, 2^nL_2 + 1)$ and size $2^{n+1}M$, where $n = 2, 3, ...$

Construction (iii): From matrix B in eqn. 3, if we construct a matrix A as $A = [B_L\ B_R]$ where

$$\text{the } j\text{th entry of } B_L \text{ is } \begin{bmatrix} B_{i,j} & B_{i,j} \\ -B_{i,j} & B_{i,j} \end{bmatrix}$$

$$\text{and the } j\text{th entry of } B_R \text{ is } \begin{bmatrix} -B_{i,j} & B_{i,j} \\ B_{i,j} & B_{i,j} \end{bmatrix}$$

then A is a ZCZ-(($2L_1$, $2N * 2L_2$), M, ($2L_1$, $L_2 + 1$)) set. Moreover A is also a mutually orthogonal complementary array set, containing M sets, each set have $2N$ arrays of order $2L_1 \times 2L_2$. We can also construct recursively a new ZCZ set A_n from A_{n-1}, where $A_0 = A$, $n = 1, 2, ...,$ thus A_n is a ZCZ-(($2^{n+1}L_1$, $2^{n+1}N * 2^{n+1}L_2$), M, ($2^{n+1}L_1$, $2^nL_2 + 1$)) set with $Z_{cz} = (2^{n+1}L_1, 2^nL_2 + 1)$ and the same size M.

Illustrative example: We conclude with an illustrative example ZCZ-((4, 32), 4, (4, 5)).

(i) We construct a mutually orthogonal complementary array set B with four arrays (refer to [3]):

$$B_{11} = \begin{bmatrix} + & + & + & - \\ + & + & + & - \\ + & - & + & + \\ - & + & - & - \end{bmatrix} B_{12} = \begin{bmatrix} + & + & + & - \\ - & - & - & + \\ + & - & + & + \\ + & - & + & + \end{bmatrix}$$

$$B_{21} = \begin{bmatrix} + & + & - & + \\ + & + & - & + \\ + & - & - & - \\ - & + & + & + \end{bmatrix} B_{22} = \begin{bmatrix} + & + & - & + \\ - & - & + & - \\ + & - & - & - \\ + & - & - & - \end{bmatrix}$$

(ii) Using construction (i), we can derive the following ZCZ array set A ZCZ-((4, 32), 4, (4, 5)) with $Z_{cz} = (4, 5)$ and size $M = 4$,

$$A = \begin{bmatrix} A^{(1)} \\ A^{(2)} \\ A^{(3)} \\ A^{(4)} \end{bmatrix} \begin{aligned} A^{(1)} &= \left[B_{11}B_{11}\ B_{12}B_{12}\ (-B_{11})B_{11}\ (-B_{12})B_{12}\right]_{4\times 32} \\ A^{(2)} &= \left[B_{21}B_{21}\ B_{22}B_{22}\ (-B_{21})B_{21}\ (-B_{22})B_{22}\right]_{4\times 32} \\ A^{(3)} &= \left[(-B_{11})B_{11}\ (-B_{12})B_{12}\ B_{11}B_{11}\ B_{12}B_{12}\right]_{4\times 32} \\ A^{(4)} &= \left[(-B_{21})B_{21}\ (-B_{22})B_{22}\ B_{21}B_{21}\ B_{22}B_{22}\right]_{4\times 32} \end{aligned}$$

In addition, we can construct a class of ZCZ-((4, 2^{2n+5}), 2^{n+2}, (4, $2^{n+2} + 1$)) set with $Z_{cz} = (4, 2^{n+2} + 1)$ and size 2^{n+2} by using construction (ii); a class of ZCZ-((2^{n+3}, 2^{2n+5}), 2, (2^{n+3}, $2^{n+2} + 1$)) set with $Z_{cz} = (2^{n+3}, 2^{n+2} + 1)$ and size 2 by using construction (iii). By considering the transposition matrix, the ZCZ-((2^{2n+5}, 4), 2^{n+2}, ($2^{n+2} + 1$, 4)) set with $Z_{cz} = (2^{n+2} + 1, 4)$ and size 2^{n+2} and ZCZ-((2^{2n+5}, 2^{n+3}), 2, ($2^{n+2} + 1$, 2^{n+3})) set with $Z_{cz} = (2^{n+2} + 1, 2^{n+3})$ and size 2 can also be obtained.

It should be noted that the idea presented in this Letter can also be extended to a three-dimensional code set with cuboid zero correlation zone. A four- or higher-dimensional ZCZ code construction is also possible, although no obvious geometrical sense exists.

Acknowledgment: The authors would like to thank the National Science Foundation of China (NSFC) under Grant No. 69825102 and 69931050, National 863 Research Project of China, and the MEXT Project of Japan, for supporting the work.

17 April 2001

Electronics Letters Online No: 20010576

DOI: 10.1049/el:20010576

X.H. Tang and P.Z. Fan (*Institute of Mobile Communications, Southwest Jiaotong University, Chengdu, Sichuan 610031, People's Republic of China*)

E-mail: xhutang@sina.com

D.B. Li (*Department of Information Engineering, Beijing University of Post and Telecommunications, People's Republic of China*)

N. Suehiro (*Graduate School of Systems & Information Engineering, Tsukuba University, Japan*)

References

1 FAN, P.Z., SUEHIRO, N., KUROYANAGI, N., and DENG, X.M.: 'A class of binary sequences with zero correlation zone', *Electron. Lett.*, 1999, **35**, (10), pp. 777–779

2 FAN, P.Z., and HAO, L.: 'Generalized orthogonal sequences and their applications in synchronous CDAM system', *IEICE Trans. Fundam. Electron. Commun. Comput. Sci.*, 2000, **E83-A**, (11), pp. 1–16

3 LÜKE, H.D.: 'Sets of one and higher dimensional welti codes and complementary codes', *IEEE Trans. Aerosp. Electron. Syst.*, 1985, **AES-21**, (2), pp. 170–179

High sensitivity waveform measurement with optical sampling using quasi-phasematched mixing in $LiNbO_3$ waveguide

S. Kawanishi, T. Yamamoto, M. Nakazawa and M.M. Fejer

High efficiency ($1.7 \times 10^{-2}\,W^{-1}$) waveform measurement is experimentally demonstrated using quasi-phasematched mixing in an $LiNbO_3$ waveguide. A 160 Gbit/s optical waveform is observed with temporal resolution of 3.6 ps.

Introduction: Optical waveform measurement by optical sampling based on optical nonlinearity is a promising method for evaluating ultrahigh-speed optical time-division multiplexed (TDM) transmissions systems [1, 2] because of its high temporal resolution [3 – 9]. Previously, we measured the waveforms of over 100 Gbit/s optical TDM signals by using sum frequency generation (SFG) in nonlinear organic crystal [3]. The SFG conversion efficiencies for the organic crystal was 3×10^{-4} W^{-1}.

Quasi-phasematched mixing (QPM) in periodically-poled $LiNbO_3$ (PPLN) is attracting interest for nonlinear material because it has high conversion efficiency [10] with negligible additive noise. Nogiwa *et al.* reported the optical sampling based on SFG in a bulk PPLN crystal with efficiency of 4.3×10^{-3} W^{-1} [4]. Higher conversion efficiency is expected by using a waveguide structure of the PPLN device [5]. In optical sampling based on SFG in a PPLN device, the wavelength of the sampling pulse should be precisely tuned to satisfy the phase-matching condition and the wavelength tolerance of the sampling pulse was ~1 nm. However, in cascaded second-order nonlinear frequency mixing ($\chi^{(2)} : \chi^{(2)}$ mixing), the wavelength of the sampling pulse is fixed and the phase-matching condition is satisfied over a 60 nm bandwidth for the optical signal [10]. We have used this $\chi^{(2)} : \chi^{(2)}$ mixing in a PPLN waveguide for a 100 Gbit/s all-optical time-division multiplexing experiment [11]. In this Letter, high efficiency waveform measurement is successfully demonstrated using QPM in a low loss (3 dB) $LiNbO_3$ PPLN waveguide. The total fibre-to-fibre conversion efficiency was 1.7×10^{-2} W^{-1}. The waveform of 160 Gbit/s optical TDM signal was measured with temporal resolution of 3.6 ps.

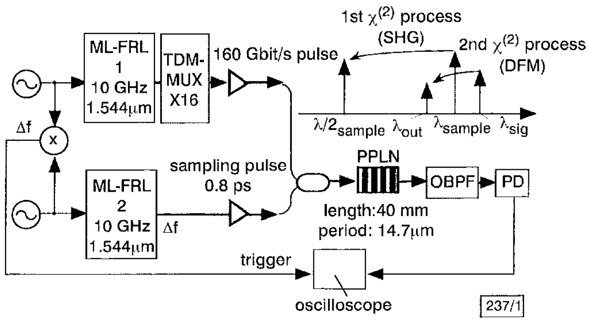

Fig. 1 *Schematic diagram of optical sampling using QPM in PPLN*

Experiment: The experimental setup is shown in Fig. 1. A 10 GHz, optical TDM signal pulse was generated by a modelocked fibre ring laser (ML-FRL). It was then multiplexed in the time domain by a planar-lightwave circuit (PLC) to produce a 160 Gbit/s signal. The optical sampling pulse was generated by a 0.8 ps, 1550 nm wavelength ML-FRL. They were combined and introduced to the PPLN waveguide. The PPLN waveguide used in this experiment was a 40 mm-long waveguide with a domain inversion period of 14.7 μm. In this device, a cascaded $\chi^{(2)}$ process generated the output light. The principle of the cascaded $\chi^{(2)}$ process is also shown in Fig. 1. The second harmonic (SH) of the 1550 nm sampling pulse is generated; simultaneously this SH pulse and the signal pulse generate an output pulse at their difference frequency through difference-frequency mixing (DFM). In the experiment, the temperature of the device was set to 80°C to avoid photorefractive effects. The output of the PPLN waveguide was filtered to remove the sampling and signal component and detected by a photodetector. The output electrical signal was displayed on an oscilloscope triggered by the frequency difference component Δf between the oscillators that drove the two ML-FRL.

Fig. 2*a* shows the measured output power of the converted light as a function of input signal power. The device was first characterised with two continuous wave light sources for the sampling and signal light in this measurement. As shown in the Figure, the output power is proportional to the input signal light power. The calculated fibre-to-fibre conversion efficiency η defined as $P_{out}/(P_{sample}P_{sig})$ where P_{out}, P_{sample}, and P_{sig} are the power of output light, input sampling light, and input signal light, respectively, was 1.7×10^{-2} W^{-1} when the P_{sample} was +14 dBm. This value is four times higher than that of the bulk PPLN [4]. Note that in a cascaded $\chi^{(2)}$ process device, the power of output light P_{out} is proportional to P_{sig}^2 instead of P_{sig}. Therefore, to compare the efficiency of a cascaded-$\chi^{(2)}$ device with that of an SFG device where P_{out} is proportional to P_{sig}, the sampling power P_{sample} in a cascaded-$\chi^{(2)}$ device should be specified. Fig. 2*b* shows the relative conversion efficiency as a function of signal wavelength. This device showed broadband characteristics from 1535 to 1600 nm and the 3 dB bandwidth was 60 nm. It should be noted that the phase matching condition was satisfied without changing the wavelength of the sampling light and therefore it is possible to perform optical sampling over a 60 nm bandwidth with a single pump wavelength. Fig. 3 shows the measured waveform of the 160 Gbit/s signal by optical sampling for the signal wavelength of 1544 nm. Waveform measurement with over 20 dB signal-to-noise ratio (SNR) was achieved in this experiment. The temporal resolution of 3.6 ps was determined by the phase mismatch of the PPLN.

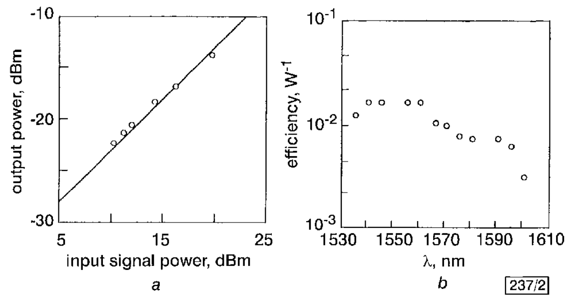

Fig. 2 *Static characteristics of PPLN*

a Input power against output power characteristics
b Wavelength characteristics

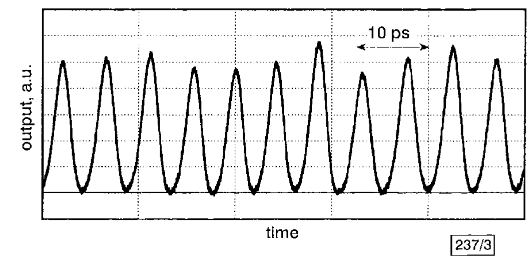

Fig. 3 *Measured 160 Gbit/s signal waveform*

Temporal resolution was 3.6 ps

Discussion: To improve temporal resolution of sampling, it is necessary to shorten the device length L. The L-dependence of the conversion efficiency η is $\eta \propto L^2$, and the L-dependence of the temporal resolution τ determined by the phase-matching bandwidth of the device for sampling pulse is $\tau \propto L$. To obtain the temporal resolution of 1 ps, the device length should be reduced to 13 mm, which would reduce the conversion efficiency 1.9×10^{-3} W^{-1}. This is still about ten times that of our previous report [3], so that optical sampling with better than 1 ps temporal resolution with high sensitivity is expected. As for the measurable wavelength range, this optical sampling system has a wide tuning range for the signal wavelength corresponding to the *C*-band and *L*-band. In this experiment, we changed the optical filter after the PPLN device for signal wavelengths shorter and longer than that of the sampling pulse. But by optimising the wavelength of the sampling pulse, it is possible to measure the waveform of both *C*-band and *L*-band signals without changing the filter, which enables realisation of a simple configuration for the optical sampling system.

Conclusion: We have shown the waveform measurement of a 160 Gbit/s signal with optical sampling using broadband, high efficiency quasi-phasematched mixing in an $LiNbO_3$ waveguide. The measurable signal wavelength region was 1535–1600 nm and the maximum conversion efficiency was 1.7×10^{-2} W^{-1}. This sampling system will realise high sensitivity waveform measurements with temporal resolution better than 1 ps for > 100 Gbit/s OTDM signals.

Acknowledgment: The authors would like to thank M. Kawachi and K.-I. Sato for their encouragement.

23 April 2001
Electronics Letters Online No: 20010565
DOI: 10.1049/el:20010565

S. Kawanishi and T. Yamamoto (*NTT Network Innovation Laboratories, 1-1, Hikari-no-oka, Yokosuka, Kanagawa 239-0847, Japan*)

E-mail: kawanisi@exa.onlab.ntt.co.jp

M. Nakazawa (*Tohoku University, 2-1-1 Katahira, Aoba-ku, Sendai-shi 980-8577, Japan*)

M.M. Fejer (*E.L. Ginzton Laboratory, Stanford University, Stanford CA 94305-4085, USA*)

References

1 KAWANISHI, S.: 'Ultrahigh-speed optical time-division-multiplexed transmission technology based on optical signal processing', *IEEE J. Quantum Electron.*, 1998, **34**, pp. 2064–2079

2 NAKAZAWA, M., YAMAMOTO, T., and TAMURA, K.R.: '1.28 Tbit/s-70 km OTDM transmission using third- and fourth-order simultaneous dispersion compensation with a phase modulator'. ECOC 2000, Tech. Dig., 2000, Paper PD-2.6

3 TAKARA, H., KAWANISHI, S., YOKOO, A., TOMARU, S., KITOH, T., and SARUWATARI, M.: '100 Gbit/s optical signal eye-diagram measurement with optical sampling using nonlinear optical crystal', *Electron. Lett*, 1996, **32**, pp. 2256–2258

4 NOGIWA, S., OHTA, H., KAWAGUCHI, Y., and ENDO, Y.: 'Improvement of sensitivity in optical sampling system', *Electron. Lett.*, 1999, **35**, pp. 917–918

5 ISHIZUKI, H., FUJIMURA, M., SUHARA, T., and NISHIHARA, H.: '$LiNbO_3$ waveguide quasi-phase-matched sum-frequency generation device for high-efficiency optical sampling', *Trans. Inst. Electron. Inf. Commun. Eng.*, 2000, **J83-C**, pp. 197–203 (in Japanese)

6 DENG, K.-L., RUNSER, R.J., GLESK, I., and PRUCNAL, P.R.: 'Single-shot optical sampling oscilloscope for ultrafast optical waveforms', *IEEE Photonics Technol. Lett.*, 1998, **10**, pp. 397–399

7 DIEZ, S., LUDWING, R., SCHMIDT, C., FEISTE, U., and WEBER, H.: '160-Gb/s optical sampling by gain-transparent four-wave mixing in a semiconductor optical amplifier', *IEEE Photonics Technol. Lett.*, 1999, **11**, pp. 1402–1404

8 KIKUCHI, K.: 'Optical sampling system at 1.5 µm using two photon absorption in Si avalanche photodiode', *Electron. Lett*, 1998, **34**, pp. 1354–1355

9 THOMSEN, B.C., BARRY, L.P., DUDLEY, J.M., and HARVEY, J.D.: 'Ultra-sensitive all-optical sampling at 1.5 µm using waveguide two-photon absorption', *Electron. Lett.*, 1999, **35**, pp. 1483–1484

10 CHOU, M.H., BRENER, I., LENZ, G., SCOTTI, R., CHABAN, E.E., SHMULOVICH, J., PHILEN, D., PARAMESWARAN, K.R., and FEJER, M.M.: 'Efficient, wideband and tunable mid-span spectral inverter using cascaded nonlinearities in $LiNbO_3$ waveguides', *IEEE Photonics Technol. Lett.*, 2000, **12**, pp. 82–84

11 KAWANISHI, S., CHOU, M.H., FUJIURA, K., FEJER, M.M., and MORIOKA, T.: 'All optical modulation and time-division-multiplexing of 100 Gbit/s signal using quasi-phasematched mixing in $LiNbO_3$ waveguides', *Electron. Lett.*, 2000, **36**, pp. 1568–1569

3.08 Tbit/s (77 × 42.7 Gbit/s) WDM transmission over 1200 km fibre with 100 km repeater spacing using dual C- and L-band hybrid Raman/erbium-doped inline amplifiers

B. Zhu, L. Leng, L.E. Nelson, Y. Qian, L. Cowsar, S. Stulz, C. Doerr, L. Stulz, S. Chandrasekhar, S. Radic, D. Vengsarkar, Z. Chen, J. Park, K.S. Feder, H. Thiele, J. Bromage, L. Gruner-Nielsen and S. Knudsen

3.08 Tbit/s (77 × 42.7 Gbit/s) WDM transmission over 1200 km fibre with 100 km amplifier spacing and 100 GHz channel spacing is demonstrated. Error-free transmission of all 77 channels is achieved by employing dual C- and L-band hybrid Raman/erbium-doped inline amplifiers, experimental low dispersion slope TrueWave® fibre, and forward error correction.

Introduction: With the increasing demand for transmission capacity on optical fibre trunk lines, ultra-long haul 40 Gbit/s per-channel all-optical transmission systems are now becoming very attractive [1 – 3], as they offer high signal spectral efficiency and large capacity with a smaller number of channels, at potentially lower cost. However, the design of typical terrestrial transmission systems at 40 Gbit/s line rate with 100 km amplifier spacing is challenging, since the launched power into both the transmission fibre and the dispersion compensating fibre (DCF) is limited owing to non-linearity related impairments. The low dispersion tolerance of 40 Gbit/s signals is also an important issue [4]. The dispersion slope of the transmission fibre and the dispersion compensating modules must be matched to yield a net accumulated dispersion of less than approximately ±30 ps/nm for all WDM channels.

In this Letter, we demonstrate transmission of 3.08 Tbit/s (77 × 42.7 Gbit/s) over 1200 km fibre with 100 km spans by employing dual C- and L-band distributed Raman amplification, experimental low dispersion slope TrueWave® fibre, and forward error correction. The 3.08 Tbit/s comprises 40 100 GHz spaced WDM channels in the C-band and 37 100 GHz spaced WDM channels in the L-band. Error-free transmission of all 77 channels is achieved. Furthermore, low dispersion slope fibre and matched DCF alleviate the need for any per-channel post-compensation in the C-band.

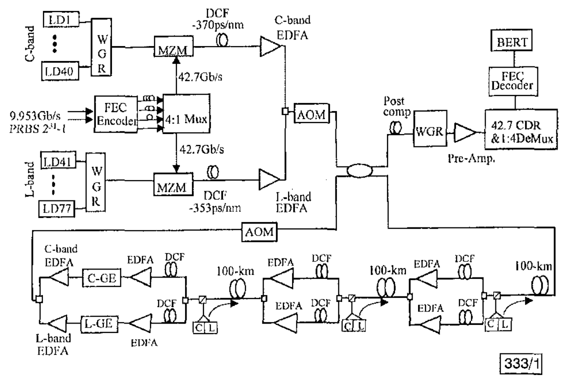

Fig. 1 *Experimental setup*

Experimental setup: Fig. 1 is a schematic diagram of the recirculating loop experimental setup. The WDM transmitters consist of 40 DFB laser diodes (LD) in the C-band (1530.72–1561.82 nm), and 37 DFB LD in the L-band (1570.42–1600.6 nm) on the 100 GHz-spaced ITU-T frequency grid. The C- and L-band channels are multiplexed separately by waveguide grating routers (WGR), and modulated by two $LiNbO_3$ Mach-Zehnder modulators (MZM) driven by 42.7 Gbit/s electrical NRZ signals. Electrical time-domain multiplexing (ETDM) is employed to generate the 42.7 Gbit/s signals from four 10.664 Gbit/s data streams, each consisting of $2^{31} - 1$ PRBS, 9.953 Gbit/s data encoded with 255/239 Reed-Solomon FEC. For pre-compensation of dispersion and channel decorrelation during transmission, the C- and L- band WDM channels are transmitted through –370 and –353 ps/nm dispersion, respectively, prior to being amplified, then combined and launched into the transmission line.

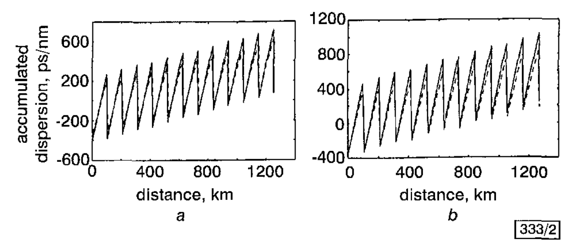

Fig. 2 *Dispersion maps for C-band and L-band*

a C-band
– · — λ = 1561.83 nm
– – – – λ = 1530.72 nm
b L-band
——— λ = 1600.6 nm
- · - - - λ = 1570.4 nm

The loop contains three 100 km spans of experimental TrueWave® fibre having a low dispersion slope and three dual C- and